Neuromyelitis Optica Immunoglobulin G Present in Sera From Neuromyelitis Optica Patients Affects Aquaporin-4 Expression and Water Permeability of the Astrocyte Plasma Membrane

Luciana Melamud,[1,2] Juan M. Fernández,[1] Valeria Rivarola,[1] Gisela Di Giusto,[1] Paula Ford,[1] Andrés Villa,[1,2] and Claudia Capurro[1]★

[1]Laboratorio de Biomembranas, Departamento de Fisiología y Biofísica, Facultad de Medicina, Universidad de Buenos Aires, Buenos Aires, Argentina
[2]Consultorio de Neuroinmunología, Centro Universitario de Neurología Dr. J.M. Ramos Mejía, Facultad de Medicina, Universidad de Buenos Aires, Buenos Aires, Argentina

NMO-IgG autoantibody selectively binds to aquaporin-4 (AQP4), the most abundant water channel in the central nervous system and is now considered a useful serum biomarker of neuromyelitis optica (NMO). A series of clinical and pathological observations suggests that NMO-IgG may play a central role in NMO physiopathology. The current study evaluated, in well-differentiated astrocytes cultures, the consequences of NMO-IgG binding on the expression pattern of AQP4 and on plasma membrane water permeability. To avoid or to facilitate AQP4 down-regulation, cells were exposed to inactivated sera in two different situations (1 hr at 4°C or 12 hr at 37°C). AQP4 expression was detected by immunofluorescence studies using a polyclonal anti-AQP4 or a human anti-IgG antibody, and the water permeability coefficient was evaluated by a videomicroscopy technique. Our results showed that, at low temperatures, cell exposure to either control or NMO-IgG sera does not affect either AQP4 expression or plasma membrane water permeability, indicating that the simple binding of NMO-IgG does not affect the water channel's activity. However, at 37°C, long-term exposure to NMO-IgG induced a loss of human IgG signal from the plasma membrane along with M1-AQP4 isoform removal and a significant reduction of water permeability. These results suggest that binding of NMO-IgG to cell membranes expressing AQP4 is a specific mechanism that may account for at least part of the pathogenic process. © 2012 Wiley Priodicals, Inc.

Key words: Devic's syndrome; primary astrocytes culture; water transport; aquaporin-4

Neuromyelitis optica (NMO) or Devic's syndrome is a devastating disease of the central nervous system (CNS) that affects mainly the optic nerves and spinal cord (Mandler et al., 1993). NMO can be distinguished from classical multiple sclerosis (MS) by clinical, neuroimaging, physiopathological, and serological criteria (Wingerchuk et al., 1999, 2006; Wingerchuk and Weinshenker, 2005). A new serum autoantibody (NMO-IgG) has recently been detected in NMO patients, becoming the first specific biomarker of an autoimmune CNS demyelinating disease (Lennon et al., 2004). NMO-IgG binds selectively to aquaporin-4 (AQP4), the most abundant water channel in the CNS, highly expressed in the polarized plasma membrane of astrocytic endfeet facing the blood—brain barrier (Nilsen et al., 1997; Verkman et al., 2006). Previous studies have shown that AQP4 is expressed as two major isoforms (M1 and M23). These isoforms aggregate to form structures known as orthogonal arrays of particles (OAPs), the size of which is determined by their concentration ratio (Verbavatz et al., 1997; Furman et al., 2003).

It is still controversial whether NMO-IgG specifically binds to OAP assemblies or M1 and/or M23 isoforms (Marnetto et al., 2009; Nicchia et al., 2009; Tani et al., 2009; Mader et al., 2010; Crane et al., 2011). Several lines of evidence indicate that NMO-IgG not only serves as a

disease marker but also plays a crucial role in the pathogenesis of NMO (Bennett et al., 2009; Bradl et al., 2009). In fact, it was recently demonstrated that binding of NMO-IgG to the extracellular domain of AQP4 reversibly down-regulates its plasma membrane expression in nonneural cells (HEK-293) transgenically expressing AQP4 (Hinson et al., 2007). Down-regulation of AQP4 has been shown to be temperature and time dependent, consistent with modulation of surface antigens through intermolecular cross-linking by divalent IgG. The authors also demonstrated that, in the presence of active complement, binding of NMO-IgG to surface AQP4 initiated strong and rapid loss of cell membrane integrity (Hinson et al., 2007). AQP4 modulation after NMO-IgG binding was also observed in primary rat astrocyte cultures, but the consequences of this binding on the AQP4-related water permeability were not evaluated (Hinson et al., 2008). However, another group proposed that NMO-IgG treatment does not significantly affect AQP4 function in astrocytes (Nicchia et al., 2009). This observation appears to contrast with that of Hinson et al. (2007, 2008) if a water channel, such as AQP4, is endocyted and degraded after NMO-IgG binding; it would be expected that membrane water permeability would be affected as previously described for other tissues (Parisi et al., 1997). Therefore, the aim of our work was to evaluate the molecular and functional consequences of NMO-IgG binding to the AQP4 on rat primary astrocytes cultures that express high levels of endogenous AQP4. In particular, we investigated how NMO-IgG binding may affect AQP4 expression as well as the astrocyte membrane water permeability. To achieve this, astrocytes were well differentiated with cAMP treatments for 7–15 days, and sera of human controls or three patients with a diagnosis of NMO were separately evaluated. Immunofluorescence techniques were used to detect AQP4 expression, either by a commercial anti-AQP4 or a human anti-IgG antibody. Cells were exposed to inactivated sera for 1 hr at 4°C (to restrict membrane fluidity) or 12 hr at 37°C, as previously described for HEK-293 cells transfected with AQP4 (Hinson et al., 2007). Our results showed that the simple exposure of astrocytes to NMO sera at 4°C does not change either the NMO-IgG signal or the plasma membrane water permeability. In contrast, at 37°C, long-term exposure to NMO sera clearly induced a loss of NMO-IgG signal from plasma membrane, along with a significant reduction of water permeability.

MATERIALS AND METHODS

Cell Cultures

Primary cultures of rat astrocytes were a generous gift from Dr. Juana Pasquini (IQUIFIB, FFyB, UBA). Cultures were obtained from cerebral hemispheres of newborn rats (0–2 days) as described by McCarthy and de Vellis (1980) and plated onto poly–L-lysine-coated Petri dishes with DMEM/Ham's F12 (1:1 v/v) containing 5 μg/ml streptomycin and 5 U/ml penicillin, supplemented with 10% fetal bovine serum

(FBS) at 37°C and 5% CO_2. Cell suspensions were seeded in poly-L-lysine-coated 75-cm^2 tissue culture flasks. After 14 days in culture, microglia was separated by shaking for 30 min in an orbital shaker at 150 rpm/min, and oligodendrocytes were separated from astrocytes by continuous shaking for 24 hr at 240 rpm/min. Astrocytes, fixed at the bottom of the flasks, were maintained for 3–4 weeks in a well-defined culture medium (DEMEM-F12 supplemented with glucose 0.4%, $NaHCO_3$ 0.24%, FBS 10% and penicillin-streptomycin). Before the experiments, astrocytes were differentiated with dibutyryl-AMPc (150 μM) for 15 days and medium was changed twice per week. The purity of the cell culture was assessed by immunofluorescence using an astrocytic marker, glial fibrilary acidic protein antibody (anti-GFAP) and oligodendorcyte antibody (anti-O4; Sigma and Chemicon, respectively). Immunocytochemistry showed that >95% of the cells stained positively for GFAP. For immunofluorescence and water permeability studies, astrocytes were seeded on glass coverslips (diameter 1.2 cm) at $5–10 \times 10^3$ cells/ml densities for 48 hr and then subjected to the different experimental conditions.

Patients and Serum Samples

Serum samples were collected from three patients with NMO from the Neuroimmunology Division of the Ramos Mejia Hospital, Argentina. All patients fulfilled the original diagnostic criteria for NMO (Wingerchuk et al., 1999) and were NMO-IgG positive as described by Saiz et al. (2007). As a control, we included serum from three healthy NMO-IgG negative volunteers. Sera were stored at −80°C, and complement was inactivated by holding for 30 min at 56°C. Before experiments, sera were preadsorbed with non-AQP-expressing rat renal cells (Blot-Chabaud et al., 1996) to reduce binding of IgG to nonneuronal antigens.

Demographic and clinical characteristics of patients included in our study are shown in Table I. Median age at onset of disease was 32 years (range 19–53 years), and median time of followup was 4 years (range 1–8 years). The median time elapsed between optic neuritis and myelitis was 22 months (range 1–38 months). Kurtzke's Expanded Disease Severity Score on last visit ranged from 4 to 6.

All patients presented recurrent disease, and only one patient had been receiving azathioprine (3 mg/kg daily), for 2 years, when blood samples were drawn for this study (Table II). All subjects signed the informed consent form, and the study was approved by the Institutional Review Board and conducted in compliance with the Declaration of Helsinki.

Antibodies

Rabbit polyclonal antibody for AQP4, raised against amino acids 244–323 mapping at the C-terminus AQP4; chicken antiglial fibrillary acidic protein (GFAP); chicken anti-O4 glycoprotein; and mouse anti-β–actin were purchased from Santa Cruz Biotechnology (Santa Cruz, CA), Neuromics (Minneapolis, MN), Chemicon (Temecula, CA), and Sigma-Aldrich (St. Louis, MO), respectively. Fluorochrome-conjugated IgGs were purchased from Jackson Immunoresearch (West Grove, PA; Cy3-goat anti-rabbit IgG specific, FITC goat anti-human or rabbit anti-chicken IgG specific) and Chemicon (Cy3-donkey

TABLE I. Demographic and Clinical Characteristics of Patients With NMO

	P1	P2	P3
Sex	Female	Female	Female
Age	27	57	28
Age of onset of first event (years)	19	53	25
Ethnic origin	Caucasian	Caucasian	Caucasian
Duration of followup (years)	8	3	1
First event	Myelitis	Myelitis	Optic neuritis
Time elapsed between optic neuritis and myelitis (months)	38	1	27
Disease duration (years)	8	4	3
Annual relapse rate	0.75	2	2
Expanded disability status scale	4	5	6
Course of disease	Recurrent	Recurrent	Recurrent
Initial brain MRI	Normal	Abnormal but not suggestive of MS	Normal
Spinal cord MRI lesion > 3 segments	Yes	Yes	Yes
Oligoclonal IgG bands in the CSF	No	No	No
Associated diseases	No	Myasthenia gravis	No
Actual treatment	Azathioprine	Azathioprine	Azathioprine

TABLE II. NMO Status at the Moment of Serum Sample Extraction

	P1	P2	P3
NMO-IgG status	Positive	Positive	Positive
NMO status disease	Remission	Remission	Relapsing
Steroid treatment	No	No	No
Immunosuppressive treatment	Yes	No	No

anti-chicken IgG). Horseradish peroxidase-conjugated goat anti-rabbit and anti-mouse immunoglobulins were purchased from Sigma-Aldrich and Jackson Immunoresearch, respectively.

Astrocytes Pretreatment With Control or Patient Sera

Astrocytes were exposed to control or patient sera (dilution 1/50 in culture media) for 1 hr at 4°C or 12 hr at 37°C. These conditions were selected to avoid or to facilitate AQP4 down-regulation, respectively, as previously described in HEK-293 cells (Hinson et al., 2007). After these treatments, cells were washed with PBS, and then immunofluorescence staining, Western blotting, or water permeability studies were performed.

Immunofluorescence Studies

For rat AQP4, GFAP, or O4 staining, cells were fixed in 4% paraformaldehyde for 1 hr and then permeabilized with 1% glycine and 0.1% Triton X-100 at room temperature. Samples were blocked with 5% FBS for 2 hr, sequentially incubated with primary antibodies (AQP4 1/300, GFAP 1/500, or O4 1/200) overnight at 4°C and secondary antibodies for 2 hr at room temperature. For human IgG staining, sera-treated live cells were exposed to anti-IgG FITC-conjugated secondary antibodies for 1 hr and then fixed with chilled 95% ethanol/5% acetic for 15 min. After immunostaining, nuclei were stained with Hoechst (5 μg/ml) or propidium iodide (2 μg/ml). Coverslips were mounted with Vectashield mounting medium.

Images were captured using epifluorescence in an Olympus BX50 microscope or a confocal Nikon C1 micro-scope and digitalized. Fluorescence intensity was evaluated per cell, identified by nuclei staining. Ten fields were analyzed per experiment (4–12 experiments) and quantified by densito-metric analysis in ImageJ sofware.

Cell Surface Biotinylation Assay and Western Blot Studies

After serum pretreatment, 90–95%-confluent primary cultured astrocytes were washed three times in cold PBS, and cell surface biotinylation was performed with a Cell Surface Protein Isolation kit (Pierce, Roc kford, IL) following the man-ufacturer's instructions. Briefly, the cells were rinsed with PBS and then biotinylated using EZ-Link Sulfo-NHS-SS-Biotin (Pierce) in PBS for 30 min on ice. After quenching, the cells were harvested and solubilized in Lysis Buffer (Pierce) and incubated for 30 min on ice. After centrifugation at $10,000g$ for 2 min at 4°C, the supernatant was added to Immobilized Neu-trAvidin gel (Pierce) and incubated for 60 min at room temper-ature. After washing, the biotinylated proteins were eluted in SDS/PAGE sample buffer containing 50 mM dithiothreitol.

The biotinylated plasma membrane proteins were sub-ject to 12% SDS-polyacriylamide minigel electrophoresis using the Tris-Tricine buffer system (Rivarola et al., 2010) and transferred to nitrocellulose sheets (Mini Protean II; Bio-Rad, Hercules, CA). Blots were blocked with 1% bovine serum albumin in PBS-T (80 mM Na_2HPO_4, 20 mM NaH_2PO_4, 100 mM NaCl, and 0.1% Tween 20, pH 7.5) for 1 hr and incubated with anti-AQP4 overnight at 4°C (1/1,000 dilu-tion) or anti-β-actin (1/2,000 dilution) for 1 hr at 25°C. The blots were then washed and incubated with horseradish peroxidase-conjugated goat anti-rabbit or anti-mouse immu-noglobulin (1/25,000 dilution), respectively, for 1 hr at 25°C. Membranes were visualized using the chemiluminescence method (SuperSignal Substrate; Pierce) and captured on a Gbox (Syngene, Frederick, MD). Bands corresponding to AQP4 or β-actin proteins were quantitated by densitometric analysis using Gel-Pro Analyzer software (Media Cybernetics, Bethesda, MD) and expressed as the AQP4/β-actin ratio.
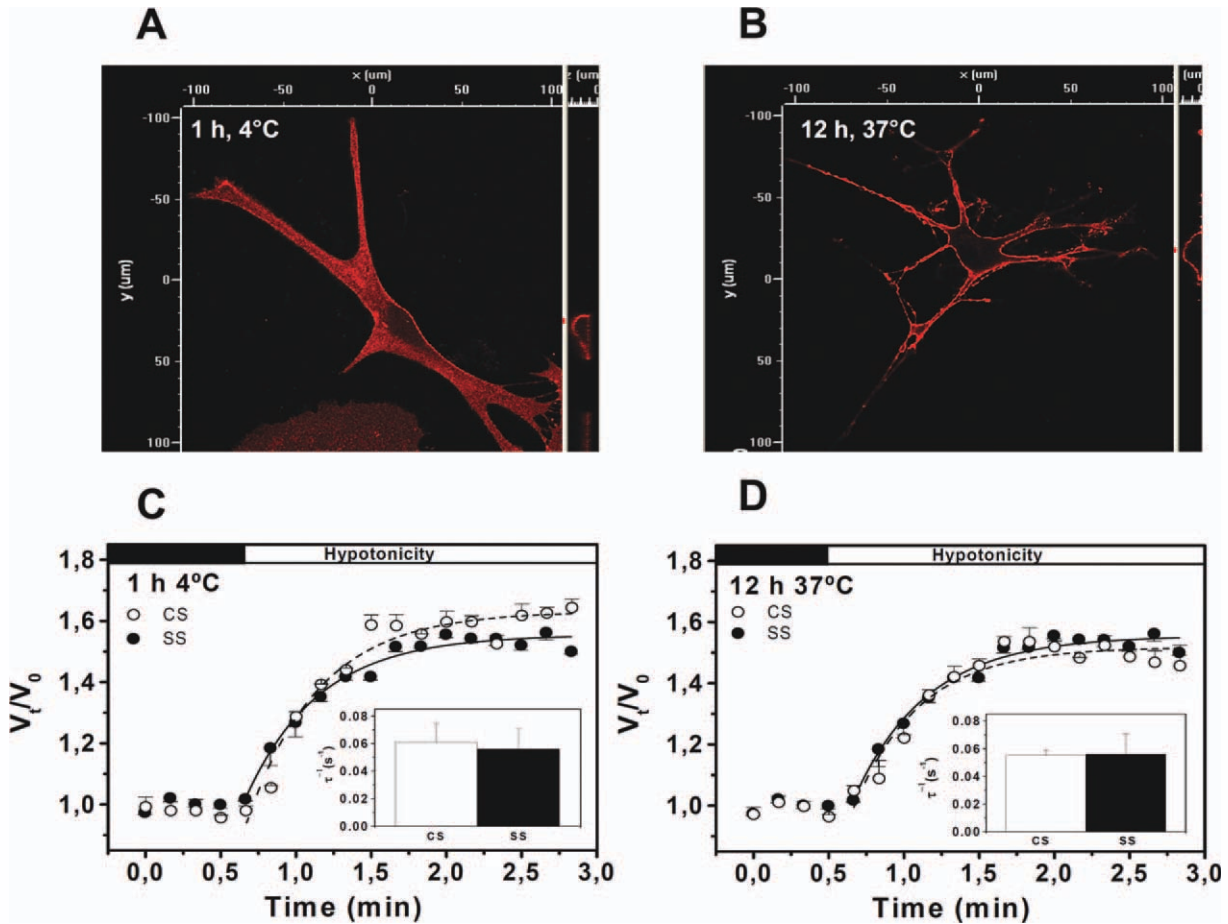
Fig. 1. Effect of control serum on AQP4 expression and membrane water permeability of astrocytes. Differentiated astrocytes were incubated with control sera (dilution 1/50) for 1 hr at 4°C or 12 hr at 37°C, and then immunofluorescence studies using a polyclonal rat anti-AQP4 antibody and the membrane water permeability were evaluated. **A,B:** Confocal microscopic analysis of xy, xz, and yz illustrating AQP4 staining at the astrocyte plasma membrane under both conditions. **C,D:** Time course of the relative cell volume (V_t/V_0) after exposure of cells to a hypotonic gradient ($\Delta OsM = 100$ mOsM) in astrocytes treated with control serum (CS) or with a standard saline solution (SS). **Insets** illustrate the time constant (τ^{-1}), assumed as the osmotic water permeability. Values are the mean ± SEM for five to eight experiments. [Color figure can be viewed in the online issue, which is available at wileyonlinelibrary.com.]

Cell Volume Changes and Osmotic Water Permeability

Primary culture astrocytes grown on coverslips were mounted on a chamber and loaded with 12 μM 2′,7′-bis(2-carboxyethyl)-5(6)-carboxyfluorescein-acetoxymethylester (BCECF-AM; Molecular Probes, Eugene, OR) for 40 min at 20°C. The chamber was then placed on the stage of a Nikon TE-200 epifluorescence inverted microscope (Nikon Planfluor ×40 oil immersion objective lens) as previously described (Ford et al., 2005). Fluorescence intensity was recorded by exciting BCECF at the isosbestic point (440 nm), where the fluorochrome is pH insensitive. Fluorescence data were acquired every 10 sec using a charge coupled device camera (Hamamatsu C4742-95) connected to a computer and the Metafluor acquisition program (Universal Imaging Corporation, Downington, PA). The procedure to estimate cell water volume was similar to the one described by Alvarez-Leefmans et al. (2006) for neuroblastoma and neuroblastoma glioma cells. The change in cell water volume can be calculated as follows:

$$\frac{V}{V_0} = \frac{\left(\frac{F_0}{F_t}\right) - f_b}{1 - f_b}$$

where V is the cell volume at time t; V_0 is V when $t = 0$; F_0 represents the signal obtained from a small region of the cell (pinhole) equilibrated with isotonic medium having an osmolality, OsM_0; F_t is the fluorescence from the same region at time $= t$ in a solution having an osmolality, OsM_t, and f_b is the relative background. This parameter corresponds to the y intercept of a plot of F_0/F_t vs. OsM_0/OsM_t, which is the relative fluorescence when no osmolality change is performed. The time course of V_t/V_0 for each experiment was fitted with a single exponential function from which the time constant (τ) was obtained. This time constant is related to the osmotic water permeability (P_f) by the following expression:

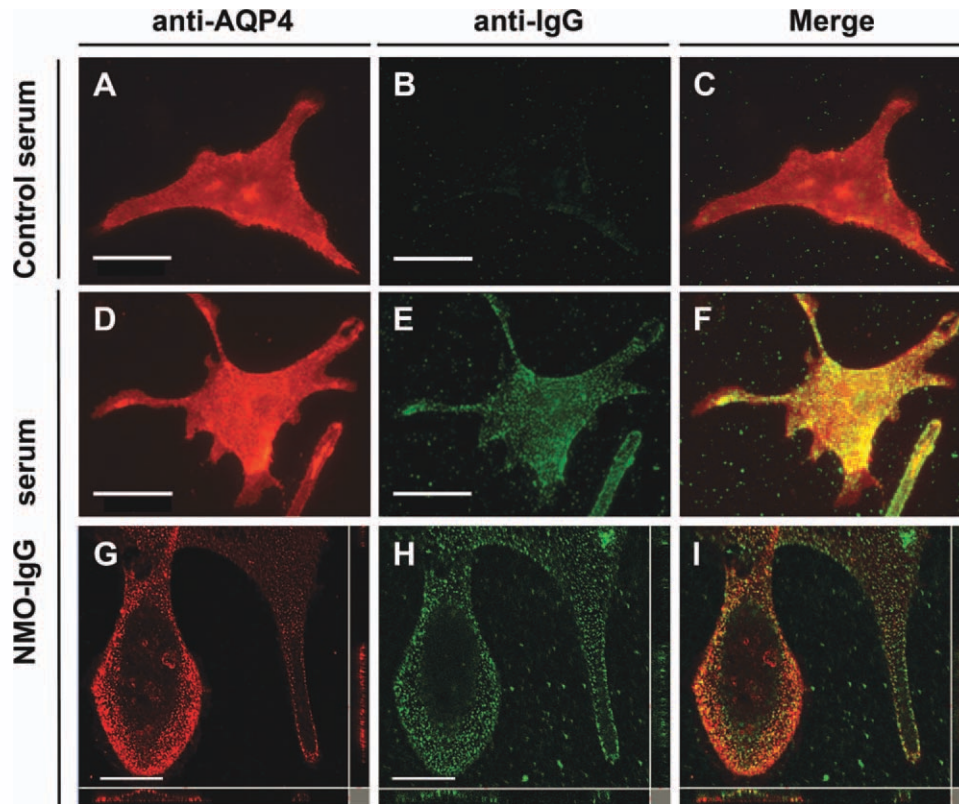$$P_f = \frac{V_0}{\tau . A . \Delta OsM . V_w}$$

Fig. 2. AQP4 expression and NMO-IgG binding in well-differentiated astrocytes. Astrocytes were first exposed to control or to NMO-IgG sera, for 1 hr at 4°C, and then double immunofluorescence experiments were performed using a polyclonal anti-AQP4 antibody (red) and anti-human IgG antibody (green). **A,D,G:** Images illustrating AQP4 staining using an anti-AQP4 antibody in astrocytes exposed either to control sera (A) or to NMO-IgG sera (D,G). **B,E,H:** Images depicting NMO-IgG signal using an anti-human IgG antibody in astrocytes exposed either to control sera (B) or to NMO-IgG sera (E,H). **C,F,I:** Merged images of AQP4 staining and NMO-IgG signal. **A–F:** Epifluorescence microscopic images. **G–H:** Confocal images. Scale bars = 20 μm.

where V_0 is the initial cell volume, A is the cell surface area, ΔOsM is the osmotic gradient, and V_w is the partial molar volume of water (18 cm^3/mol). Because of the complex geometry of astrocytes, it is not possible to obtain a value for surface volume to surface ratio, so τ^{-1} was used directly as an estimation of P_f.

Cells were incubated in an isosmotic solution (osmolality 294 ± 10 mOsM) containing (in mM): 70 NaCl, 5.5 KCl, 2.5 CaCl$_2$, 1.25 MgCl$_2$, 100 mannitol, 20 Hepes, 10 glucose. Hypotonic solutions were prepared by mannitol subtraction to obtain the desired osmolality, thus maintaining the ionic strength. Osmolalities of solutions were routinely measured in a pressure vapor osmometer (Vapro; Wescor, Logan, Utah).

RESULTS

AQP4 Expression and Functionality Are Not Affected by Exposure to Control Human Sera

Before studying the consequences of NMO-IgG binding to the endogenous AQP4 expressed in primary rat astrocytes, we evaluated the molecular and functional characteristics of this cell model when exposed to control serum for 1 hr at 4°C or 12 hr at 37°C. Immunofluorescence studies performed using an AQP4 commercial antibody showed that, as demonstrated previously, this water channel is largely expressed. Confocal microscopy analysis illustrates that, after exposure to control sera for 1 hr at 4°C (Fig. 1A) or 12 hr at 37°C (Fig. 1B), AQP4 remains selectively localized on the astrocytes plasma membrane.

Figure 1C,D shows the time course of the relative cell volume (V_t/V_0), measured in response to a hypotonic gradient (100 mOsM mannitol), and the time constant (τ) of volume changes. Because of the complex and heterogeneous morphology of astrocytes, the surface area is very difficult to calculate, so τ^{-1} was assumed to be the water permeability coefficient as previously described (Nicchia et al., 2000). Average time constant τ^{-1} for the change in cell volume was not significantly different in cells treated with control serum for 1 hr at 4°C or 12 hr at 37°C compared with cells treated with a standard saline solution (Fig. 1C,D, insets). These results demonstrate that no control serum component affects either AQP4 expression or the functionality of this water channel.

NMO-IgG Binding Modulates Endogenous AQP4 Expressed in the Astrocytes Plasma Membrane

It was reported that NMO-IgG may induce AQP4 internalization in HEK-293 cells transfected with AQP4

or in undifferentiated rat astrocytes (Hinson et al., 2007, 2008). In this study, we analyzed the consequences of NMO-IgG binding on AQP4 expressed in well-differentiated astrocytes, which conserve the in vivo morphology, after exposure to sera from control or from patients with NMO. Double-immunofluorescence experiments showed that, after exposure of cells for 1 hr at 4°C to control serum, AQP4 was largely labeled with the anti–AQP4 antibody (Fig. 2A), but no staining was revealed in the presence of anti-human IgG (Fig. 2B). In contrast, after exposure to serum containing NMO-IgG, a similar stain of the astrocytes plasma membrane was observed in experiments performed either with anti-AQP4 or with anti-human IgG antibodies (Fig. 2D–F). Furthermore, confocal images show that in this condition signals detected with both antibodies colocalize at the plasma membrane (Fig. 2G–I). These results strongly suggest that in astrocytes NMO-IgG serum specifically recognizes AQP4.

We then evaluated the consequences of NMO-IgG binding to cells exposed to each patient's serum either for 1 hr at 4°C or for 12 hr at 37°C, and the stain was densitometrically quantified. Figure 3A shows that, after 1 hr of astrocytes exposure, no staining was observed with control serum, whereas NMO-IgG resulted in a marked membrane staining (green) for all patients. In contrast, long-term (12 hr) exposure to sera from NMO patients resulted in an almost complete disappearance of cell membrane signals in all cases. Figure 3B shows the quantification of all images and illustrates that, after 1 hr of sera exposure, although staining varies among patients, it was always significantly greater compared with control serum (background). In contrast, no significant differences in staining were observed between control or NMO sera when exposure was longer (12 hr; Fig. 3C). These results suggest that NMO-IgG target was removed from the plasma membrane after long-term exposure to sera. However, immunofluorescence studies using a polyclonal anti–AQP4 antibody show that, after long-term NMO-IgG serum exposure, abundant AQP4 expression was still observed at the plasma membrane, but with a changed staining pattern. It can be noted that the laminar and continuous AQP4 signal, which is conserved after control sera exposure (Fig. 4A), had a point-shaped staining pattern after NMO-IgG treatment (Fig. 4B). This immunofluorescence stain was observed with all patients' sera.

We also investigated the identity of AQP4 affected by long-term NMO-IgG exposure. Accordingly, after cell exposure to control or patient sera for 12 hr at 37°C, cell surface proteins were biotinylated and separated with NeutrAvidin gel. Biotinylated AQP4 was analyzed by Western blot. A significant reduction in M1-AQP4 signal in biotinylated plasma membranes was observed after NMO-IgG serum exposure compared with control sera. No differences in M23-AQP4 signals were observed (Fig. 4C). These results indicate that long-term sera exposure affects AQP4 expression, the M1-AQP4 isoform being removed from the plasma membrane.
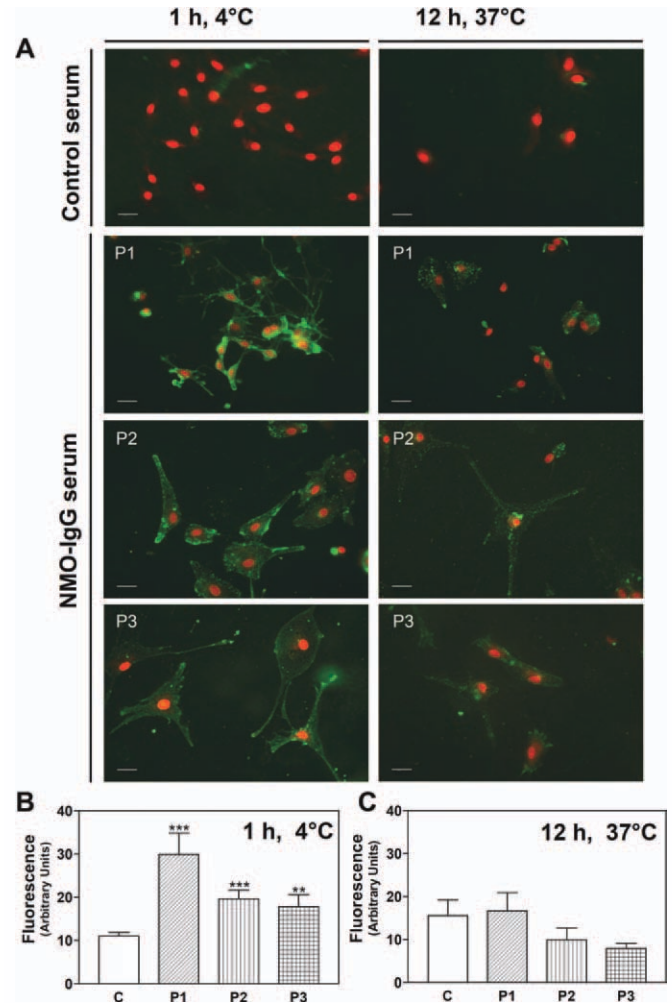

Fig. 3. Immunofluorescence studies in astrocytes exposed to control or patient sera. Astrocytes were first pretreated with control serum (C) or with three different NMO-IgG sera (P1–P3), for 1 hr at 4°C or 12 hr at 37°C, and then immunofluorescence experiments were performed using an anti-human IgG antibody (green). **A:** Representative images of astrocytes illustrating that NMO-IgG signal (P1, P2, or P3) is lost in cells exposed to NMO patient sera for 12 hr at 37°C. **B,C:** Average fluorescence of positively stained cells after 1 hr at 4°C or 12 hr at 37°C of sera exposure. Values are the mean ± SEM for four to 12 experiments for each condition (10 fields were analyzed per experiment). **$P < 0.01$, ***$P < 0.001$ control vs. NMO-IgG sera, Student's t-test for unpaired data. Scale bars = 25 μm.

Long-Term NMO-IgG Binding to AQP4 Decreases Astrocyte Plasma Membrane Water Permeability

Finally, we determined the consequences of NMO-IgG binding on cell membrane water permeability. For this purpose, we measure the time course of astrocyte swelling (V_t/V_0) in response to an osmotic gradient. Figure 5A shows that exposure of astrocytes to control or NMO-IgG serum for 1 hr at 4°C does not affect the kinetics of V_t/V_0, which results in no changes in the osmotic water permeability (Fig. 5B). In contrast,
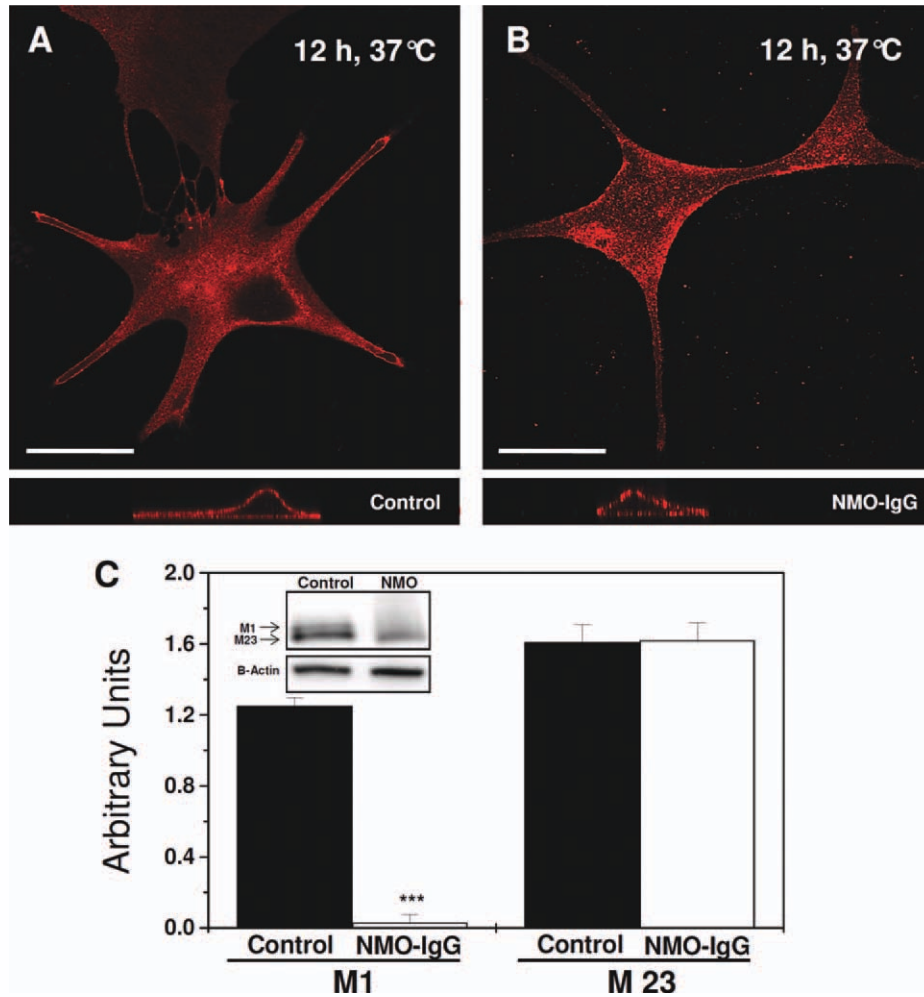
Fig. 4. AQP4 expression in plasma membrane astrocytes after exposure to control or patient's sera. Astrocytes were first exposed to control or NMO–IgG sera for 12 hr at 37°C, and then immunofluorescence and Western blot experiments were performed using a polyclonal anti-AQP4 antibody (red). **A,B:** Confocal analysis illustrating a continuous linear staining pattern of AQP4 on the plasma membrane after exposure to control serum (A) and a point-shaped staining pattern after exposure to NMO–IgG serum (B). Images are representative of three independent experiments. **C:** Densitometric analyses of Western blot assays show the biotinylated AQP4/β-actin ratio. A significant reduction of M1-AQP4 signal in biotinylated plasma membranes of astrocytes incubated with NMO was observed compared with control sera. ***$P < 0.001$ control vs. NMO–IgG sera, Student's t-test for unpaired data. **Inset:** Representative inmmunoblot showing M1 and M23 bands corresponding to AQP4 isoforms. Images are representative of three independent experiments. Scale bars = 50 μm. [Color figure can be viewed in the online issue, which is available at wileyonlinelibrary.com.]

12 hr of exposure at 37°C to NMO–IgG, but not to control serum, significantly delayed the kinetics of V_t/V_0, which can be explained by a reduction in the osmotic water permeability (Fig. 5C,D). These results clearly show that long-term exposure to NMO–IgG serum affects the astrocyte's osmotic water permeability.

DISCUSSION

We have investigated, for the first time, the consequences of NMO–IgG binding to its antigen AQP4 on the astrocyte membrane water permeability independently of complement activation. Astrocytes grown in culture lose their characteristic in vivo star-like shape as well as their AQP4 continuous plasma membrane localization (Nicchia et al., 2008), so we used cAMP to dif-ferentiate astrocytes better and, thus, ensure functional AQP4 expression in the plasma membrane. We show that, at low temperature, when the membrane fluidity and metabolic processes are restricted, exposure of cells to control or NMO–IgG sera does not affect either AQP4 expression or plasma membrane water permeability. However, long-term exposure to NMO–IgG at 37°C induced a loss of human IgG signal from the plasma membrane along with changes in the pattern of expression of AQP4 and a significant reduction in the water permeability. This AQP4 down–regulation is in line with that reported for nonneural cells transgenically expressing AQP4 and for rat undifferentiated astrocytes (Hinson et al., 2007, 2008). Nevertheless, the observed reduction of water permeability seems to contrast with
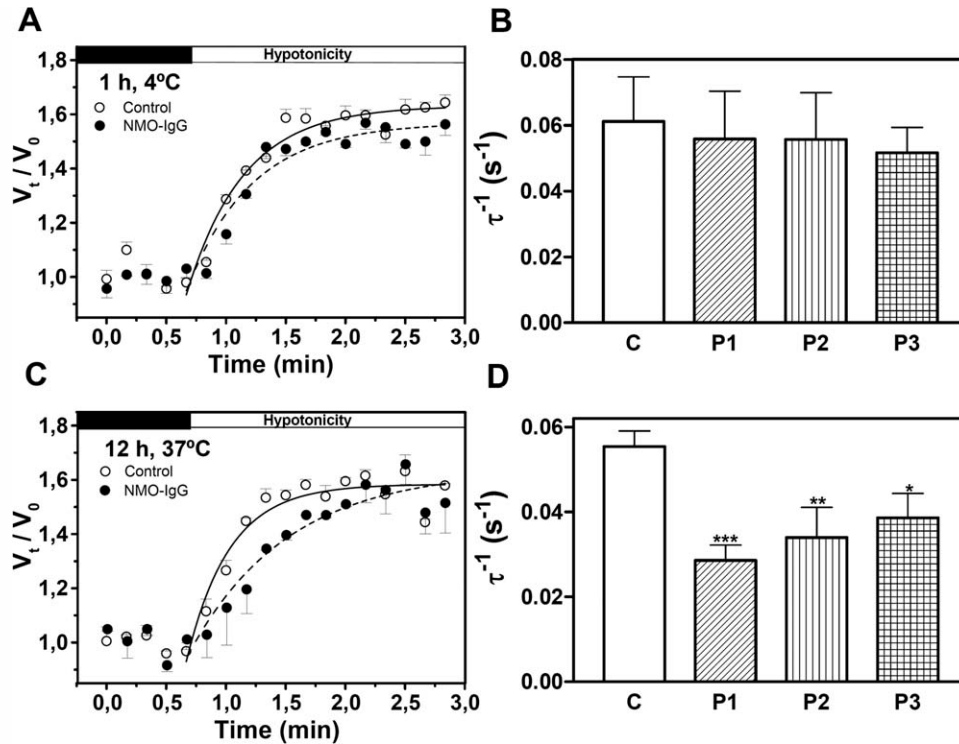
Fig. 5. Membrane water permeability of astrocytes after exposure to control or patient sera. Astrocytes were first exposed to control or NMO-IgG sera, and then the osmotic water permeability was evaluated. **A,C:** Representative time course of the relative cell volume changes (V_t/V_0) of astrocytes in response to hypotonic shock (ΔOsM = 100 mOsM) after 1 hr at $4°$C exposure to control or NMO-IgG sera (A) or 12 hr at $37°$C exposure to control or NMO-IgG sera (C). **B,D:** Membrane water permeability estimated as the time constant of cell volume changes (τ^{-1}) under the experimental conditions described for A,C, respectively. Values are the mean $\pm$ SEM for five to nine experiments. $*P < 0.05$, $**P < 0.01$, $***P < 0.001$ control vs. NMO-IgG, Student's t-test for unpaired data.

the results reported by Nicchia et al. (2009) showing that long-term exposure of rat astrocytes to NMO serum (1–2 days) did not affect the function of the AQP4 water channel. These differences may be explained either by the fact that the authors used four pooled NMO sera, probably with different antibody titers, minimizing the effects, or by the temperature at which cells were exposed to sera, which could have been different from that used in our study.

All the studies published in the past few years clearly indicate that NMO-IgG binds AQP4; however, it is yet not clear whether the target of NMO-IgG is M1, M23, or both. It was reported, from studies using immunofluorescence techniques, that epitopes of M23 would be the primary targets of NMO-IgG antibodies in HEK-293 cells expressing M1 or M23 human AQP4 isoforms (Tani et al., 2009; Mader et al., 2010). In contrast, Marnetto et al. (2009) described, from immunoprecipitation assays, how NMO-IgG recognizes the M1-AQP4 isoform of mouse kidney. It has also been shown, by double-immunofluorescence and immunoprecipitation studies, that NMO antibodies recognizes M1-AQP4 in astrocyte primary cultures as well as in HeLa cells were stably transfected with M1- and/or M23-AQP4 isoforms (Nicchia et al., 2009; Rossi et al., 2010).

Recently, Crane et al. (2011) measured the binding affinity of NMO-IgG antibodies to AQP4 in human astrocyte-derived U87MG cells expressing M1 and/or M23 or M23 mutants. The authors concluded that, although NMO-IgG can bind both isoforms, there is a greater affinity for M23- than for M1-AQP4.

All these studies support the idea that NMO-IgG could bind M1- and/or M23-AQP4 isoforms. Our studies do not attempt to clarify this point; however, even if we cannot fully discard the possibility that NMO-IgG antibody can bind to both isoforms, after long-term exposure, only M1-AQP4 is removed from astrocyte plasma membranes. A significant reduction of the water permeability was observed under this condition, suggesting that the pool of AQP4 removed from the plasma membrane significantly contributes to water transport in these cells.

Thus, we propose that water permeability reduction after NMO-IgG binding, independently of complement activation, would have a role in the development of the disease. In line with this, pathogenic roles for NMO-IgG, different from complement activation, have been suggested. For instance, it was speculated that down-regulation of AQP4 and associated proteins, such as potassium channel and glutamate transporters, could lead to impairment of extracellular fluid and potassium

homeostasis in the CNS (Hinson et al., 2008; Rash, 2009). If we assume that solutes fluxes and the presence of AQPs are key elements in cell volume regulation in the physiological state (Ford et al., 2005), then it is reasonable to think that the down–regulation of all these proteins, after NMO-IgG binding, will threaten cellular homeostasis. Therefore, we suggest that NMO-IgG-induced reduction of the plasma membrane water permeability is a specific mechanism that may account for at least part of the pathogenic process.

ACKNOWLEDGMENTS

REFERENCES

Alvarez-Leefmans FJ, Herrera-Perez JJ, Marquez MS, Blanco VM. 2006. Simultaneous measurement of water volume and pH in single cells using BCECF and fluorescence imaging microscopy. Biophys J 90:608–618.

Bennett JL, Lam C, Kalluri SR, Saikali P, Bautista K, Dupree C, Glogowska M, Case D, Antel JP, Owens GP, Gilden D, Nessler S, Stadelmann C, Hemmer B. 2009. Intrathecal pathogenic antiaquaporin-4 antibodies in early neuromyelitis optica. Ann Neurol 66:617–629.

Blot-Chabaud M, Laplace M, Cluzeaud F, Capurro C, Cassingena R, Vandewalle A, Farman N, Bonvalet JP. 1996. Characteristics of a rat cortical collecting duct cell line that maintains high transepithelial resistance. Kidney Int 50:367–376.

Bradl M, Misu T, Takahashi T, Watanabe M, Mader S, Reindl M, Adzemovic M, Bauer J, Berger T, Fujihara K, Itoyama Y, Lassmann H. 2009. Neuromyelitis optica: pathogenicity of patient immunoglobulin in vivo. Ann Neurol 66:630–643.

Crane JM, Lam C, Rossi A, Gupta T, Bennett JL, Verkman AS. 2011. Binding affinity and specificity of neuromyelitis optica autoantibodies to aquaporin-4 m1/m23 isoforms and orthogonal arrays. J Biol Chem 286:16516–16524.

Ford P, Rivarola V, Chara O, Blot-Chabaud M, Cluzeaud F, Farman N, Parisi M, Capurro C. 2005. Volume regulation in cortical collecting duct cells: role of AQP2. Biol Cell 97:687–697.

Furman CS, Gorelick-Feldman DA, Davidson KG, Yasumura T, Neely JD, Agre P, Rash JE. 2003. Aquaporin-4 square array assembly: opposing actions of M1 and M23 isoforms. Proc Natl Acad Sci U S A 100:13609–13614.

Hinson SR, Pittock SJ, Lucchinetti CF, Roemer SF, Fryer JP, Kryzer TJ, Lennon VA. 2007. Pathogenic potential of IgG binding to water channel extracellular domain in neuromyelitis optica. Neurology 69:2221–2231.

Hinson SR, Roemer SF, Lucchinetti CF, Fryer JP, Kryzer TJ, Chamberlain JL, Howe CL, Pittock SJ, Lennon VA. 2008. Aquaporin-4-binding autoantibodies in patients with neuromyelitis optica impair glutamate transport by down-regulating EAAT2. J Exp Med 205:2473–2481.

Lennon VA, Wingerchuk DM, Kryzer TJ, Pittock SJ, Lucchinetti CF, Fujihara K, Nakashima I, Weinshenker BG. 2004. A serum autoantibody marker of neuromyelitis optica: distinction from multiple sclerosis. Lancet 364:2106–2112.

Mader S, Lutterotti A, Di Pauli F, Kuenz B, Schanda K, Aboul-Enein F, Khalil M, Storch MK, Jarius S, Kristoferitsch W, Berger T, Reindl M. 2010. Patterns of antibody binding to aquaporin-4 isoforms in neuromyelitis optica. PLoS One 5:e10455.

Mandler RN, Davis LE, Jeffery DR, Kornfeld M. 1993. Devic's neuromyelitis optica: a clinicopathological study of 8 patients. Ann Neurol 34:162–168.

Marnetto F, Hellias B, Granieri L, Frau J, Patanella AK, Nytrova P, Sala A, Capobianco M, Gilli F, Bertolotto A. 2009. Western blot analysis for the detection of serum antibodies recognizing linear aquaporin-4 epitopes in patients with neuromyelitis optica. J Neuroimmunol 217:74–79.

McCarthy KD, de Vellis J. 1980. Preparation of separate astroglial and oligodendroglial cell cultures from rat cerebral tissue. J Cell Biol 85:890–902.

Nicchia GP, Frigeri A, Liuzzi GM, Santacroce MP, Nico B, Procino G, Quondamatteo F, Herken R, Roncali L, Svelto M. 2000. Aquaporin-4-containing astrocytes sustain a temperature- and mercury-insensitive swelling in vitro. Glia 31:29–38.

Nicchia GP, Rossi A, Mola MG, Procino G, Frigeri A, Svelto M. 2008. Actin cytoskeleton remodeling governs aquaporin-4 localization in astrocytes. Glia 56:1755–1766.

Nicchia GP, Mastrototaro M, Rossi A, Pisani F, Tortorella C, Ruggieri M, Lia A, Trojano M, Frigeri A, Svelto M. 2009. Aquaporin-4 orthogonal arrays of particles are the target for neuromyelitis optica autoantibodies. Glia 57:1363–1373.

Nilsen TW, Grayzel J, Prensky W. 1997. Dendritic nucleic acid structures. J Theor Biol 187:273–284.

Parisi M, Amodeo G, Capurro C, Dorr R, Ford P, Toriano R. 1997. Biophysical properties of epithelial water channels. Biophys Chem 68:255–263.

Rash JE. 2009. Molecular disruptions of the panglial syncytium block potassium siphoning and axonal saltatory conduction: pertinence to neuromyelitis optica and other demyelinating diseases of the central nervous system. Neuroscience 168:982–1008.

Rivarola V, Flamenco P, Melamud L, Galizia L, Ford P, Capurro C. 2010. Adaptation to alkalosis induces cell cycle delay and apoptosis in cortical collecting duct cells: role of aquaporin-2. J Cell Physiol 224:405–413.

Rossi A, Pisani F, Nicchia GP, Svelto M, Frigeri A. 2010. Evidences for a leaky scanning mechanism for the synthesis of the shorter M23 protein isoform of aquaporin-4: implication in orthogonal array formation and neuromyelitis optica antibody interaction. J Biol Chem 285:4562–4569.

Saiz A, Zuliani L, Blanco Y, Tavolato B, Giometto B, Graus F. 2007. Revised diagnostic criteria for neuromyelitis optica (NMO). Application in a series of suspected patients. J Neurol 254:1233–1237.

Tani T, Sakimura K, Tsujita M, Nakada T, Tanaka M, Nishizawa M, Tanaka K. 2009. Identification of binding sites for anti-aquaporin 4 antibodies in patients with neuromyelitis optica. J Neuroimmunol 211:110–113.

Verbavatz JM, Ma T, Gobin R, Verkman AS. 1997. Absence of orthogonal arrays in kidney, brain and muscle from transgenic knockout mice lacking water channel aquaporin-4. J Cell Sci 110:2855–2860.

Verkman AS, Binder DK, Bloch O, Auguste K, Papadopoulos MC. 2006. Three distinct roles of aquaporin-4 in brain function revealed by knockout mice. Biochim Biophys Acta 1758:1085–1093.

Wingerchuk DM, Weinshenker BG. 2005. Neuromyelitis optica. Curr Treat Options Neurol 7:173–182.

Wingerchuk DM, Hogancamp WF, O'Brien PC, Weinshenker BG. 1999. The clinical course of neuromyelitis optica (Devic's syndrome). Neurology 53:1107–1114.

Wingerchuk DM, Lennon VA, Pittock SJ, Lucchinetti CF, Weinshenker BG. 2006. Revised diagnostic criteria for neuromyelitis optica. Neurology 66:1485–1489.